Continental Shelf Research 145 (2017) 95–108

Contents lists available at ScienceDirect

Continental Shelf Research

journal homepage: www.elsevier.com/locate/csr

Research papers

Time series pCO_2 at a coastal mooring: Internal consistency, seasonal cycles, and interannual variability

Janet J. Reimer[a], Wei-Jun Cai[a,b,*], Liang Xue[a,c], Rodrigo Vargas[d], Scott Noakes[e], Xinping Hu[f], Sergio R. Signorini[g], Jeremy T. Mathis[h], Richard A. Feely[i], Adrienne J. Sutton[i,j], Christopher Sabine[i], Sylvia Musielewicz[i,j], Baoshan Chen[a,b], Rik Wanninkhof[k]

[a] School of Marine Science and Policy, University of Delaware, Newark, DE 19716, USA
[b] Department of Marine Sciences, University of Georgia, Athens, GA 30602, USA
[c] Center for Ocean and Climate Research, First Institute of Oceanography, State Oceanic Administration, Qingdao 266061, China
[d] Department of Plant and Soil Sciences, University of Delaware, Newark, DE 19716, USA
[e] Center for Applied Isotope Studies, University of Georgia, Athens, GA 30602, USA
[f] Department of Physical and Environmental Sciences, Texas A & M University - Corpus Christi, Corpus Christi, TX 78412, USA
[g] Science Applications International Corporation, Greenbelt, MD 20771, USA
[h] NOAA Arctic Research Program, Silver Spring, MD 20910, USA
[i] Pacific Marine Environmental Laboratory, NOAA, Seattle, WA 98115, USA
[j] Joint Institute for the Study of the Atmosphere and Ocean, University of Washington, Seattle, WA 98105, USA
[k] Atlantic Oceanographic and Meteorological Laboratory, NOAA, Miami, FL 33149, USA

ARTICLE INFO

Keywords:
Ocean margin CO_2
East coast
Inorganic carbon system internal consistency

ABSTRACT

Marine carbonate system monitoring programs often consist of multiple observational methods that include underway cruise data, moored autonomous time series, and discrete water bottle samples. Monitored parameters include all, or some of the following: partial pressure of CO_2 of the water (pCO_{2w}) and air, dissolved inorganic carbon (DIC), total alkalinity (TA), and pH. Any combination of at least two of the aforementioned parameters can be used to calculate the others. In this study at the Gray's Reef (GR) mooring in the South Atlantic Bight (SAB) we: examine the internal consistency of pCO_{2w} from underway cruise, moored autonomous time series, and calculated from bottle samples (DIC-TA pairing); describe the seasonal to interannual pCO_{2w} time series variability and air-sea flux (FCO_2), as well as describe the potential sources of pCO_{2w} variability; and determine the source/sink for atmospheric pCO_2. Over the ~8.5 years of GR mooring time series, mooring-underway and mooring-bottle calculated-pCO_{2w} strongly correlate with r-values > 0.90. pCO_{2w} and FCO_2 time series follow seasonal thermal patterns; however, seasonal non-thermal processes, such as terrestrial export, net biological production, and air-sea exchange also influence variability. The linear slope of time series pCO_{2w} increases by 5.2 ± 1.4 μatm y^{-1} with FCO_2 increasing 51–70 mmol m^{-2} y^{-1}. The net FCO_2 sign can switch interannually with the magnitude varying greatly. Non-thermal pCO_{2w} is also increasing over the time series, likely indicating that terrestrial export and net biological processes drive the long term pCO_{2w} increase.

1. Introduction

The world's oceans have been estimated to take up ~30% of the atmospheric CO_2 due to fossil fuel burning and other anthropogenic influences since the onset of the Industrial Revolution (Le Quere et al., 2016; Sabine et al., 2004), which has resulted in various regional declines in seawater pH (Feely et al., 2004; Takahashi et al., 2014, 2006). Overall, pCO_{2w} changes can be caused by at least one, or a combination, of: 1) atmospheric CO_2 uptake (Sabine et al., 2004); 2) sea surface temperature (Jiang et al., 2010; Shadwick et al., 2010; Takahashi et al., 1993); 3) drainage basin hydrologic cycles (Jiang et al., 2013); 4) coastal currents due to wind and/or weather patterns (Huang et al., 2013); 5) upwelling and water mass mixing (Feely et al., 2008); and 6) *in situ* biological production, which may be enhanced by large inputs from organic matter (OM) remineralization (nutrients) in the surface or terrestrial ecosystems, thus creating a positive feedback for biological production in shallow and/or stratified coastal systems (Cai et al., 2011; Shadwick et al., 2011; Sunda and Cai, 2012).

* Corresponding author at: School of Marine Science and Policy, University of Delaware, Newark, DE 19716, USA.
E-mail address: wcai@udel.edu (W.-J. Cai).

http://dx.doi.org/10.1016/j.csr.2017.06.022
Received 7 November 2016; Received in revised form 15 June 2017; Accepted 26 June 2017
Available online 04 July 2017

Anthropogenically-driven pCO_{2w}, and subsequently carbonate chemistry, temporal perturbations super-imposed on natural cycles are causes for concern for marine life and are now the focus of numerous studies that drive governmental policy and conservation efforts directed at mitigating the harmful effects in our coastal oceans. Therefore, rigorous *in situ* monitoring programs and modeling efforts are now being employed to track the fate of CO_2 in the world's oceans; consequently, there is also need to ensure that all methods for observing CO_2 are consistent.

Mooring platforms on coastal margins have been identified as key means for monitoring changing ocean pCO_{2w} on various time scales (Michalak et al., 2011). The coastal zone and marginal seas are expected to have high pCO_{2w} variability due to terrestrial influences (Bauer et al., 2013; Cai, 2011) and could be prone to enhanced pH declines (acidification) due to large quantities of OM that are remineralized in the shallow, biologically productive waters (Cai et al., 2011). CO_2, the primary anthropogenically-derived driver of ocean acidification (OA), dynamics and variability are only just beginning to be understood in most coastal regions and margins around the world. Though there is a specific lack of understanding on the U.S. east coast (Bauer et al., 2013; Jiang et al., 2013). The complex nature of CO_2 biogeochemistry and coastal zone heterogeneity, as well as limitations in spatio-temporal coverage, make discerning the time scales and sources of CO_2 variability challenging to identify (Cai, 2011; Jiang et al., 2013, 2008b; Vandemark et al., 2011; Wang et al., 2013; Wanninkhof et al., 2015). Moored coastal time series provide high frequency temporal resolution, while cruise (underway systems and discrete water samples) observations provide complimentary horizontal and vertical spatial patterns needed to assess the aforementioned influences on CO_2 biogeochemistry in coastal waters.

Historically, cruise methods for CO_2 data collection (bottle samples and underway observations) have been in use for several decades to discern spatial patterns and variability, sometimes extrapolating to create higher temporal resolution (Takahashi et al., 1993). While higher frequency moored time series data collection has only been used over the last decade or so (Sutton et al., 2014). Since CO_2 data collection has been, and remains to be, carried out via different methods at the same site, as well as across multiple sites, it is essential to show that consistent results can be reached by all methods. Additionally, discrete water samples for dissolved inorganic carbon (DIC), pH, and total alkalinity (TA) observations are not only used as direct measures themselves, but also to calculate pCO_{2w}, often in the absence of a direct method for observing pCO_{2w}. Calculated values must also be in agreement with mooring and underway observations (Patsavas et al., 2015) not only as an independent method, but also because DIC and TA can be included in biogeochemical models to determine the relative importance and the contributions of different biogeochemical processes to overall pCO_{2w} variability (Boehme et al., 1998; Xue et al., 2016). Internal consistency checks must also be periodically made during long-term deployments to ensure that results from all methods continue to agree (Patsavas et al., 2015; Ribas-Ribas et al., 2014) so that combined datasets can increase the spatio-temporal coverage of observed marine pCO_{2w} as well as allow for the examination of the biogeochemical processes that influence variability.

The first objective is to describe seasonal to interannual variability of the moored GR pCO_{2w} time series, accompanying variables, and air-sea pCO_{2w} flux (FCO_2), as well as examine how biogeochemical and environmental influences could affect pCO_{2w} on this ocean margin. The second objective is to test the agreement, or internal consistency, between underway and discrete water bottle-calculated pCO_{2w} from cruises in the South Atlantic Bight (SAB) with a pCO_{2w} time series measured by a coastal mooring in the Gray's Reef National Marine Sanctuary. Internal consistency serves to test the validity and quality of instrumentation as well as show that the same results can be achieved through various methods. Previous validation tests have been carried out on other National Oceanographic and Atmospheric Administration (NOAA) moored autonomous pCO_{2w} ($MAPCO_2$) systems (Schar et al., 2010; Sutton et al., 2014), however, this is the first field internal consistency effort compiled from various exercises over the lifetime of a NOAA $MAPCO_2$ system for a coastal margin heavily influenced by terrestrial sources of CO_2 (Cai and Wang, 1998; Jiang et al., 2013, 2008a). $MAPCO_2$ time series are still rather new, with ≤ 10 years of available quality controlled observations in the coastal oceans; however, in some cases cruises have been collecting pCO_{2w} observations for decades longer than moorings. The broader importance of the objectives is that in the future combining results from cruises over the last few decades and moored time series with good agreement could lay the ground work for studies to discern multi-year to multi-decadal variability. Within the first objective, we also aim to determine if the site is an annual net source or sink for atmospheric CO_2, as coastal margins represent highly biologically and socio-economically important regions that could be impacted by increased atmospheric CO_2 uptake. The GR mooring is one of the few coastal CO_2 time series that provides an important opportunity to compare pCO_{2w} measured from a coastal margin $MAPCO_2$ system to underway and discrete water samples, as well as a describe a continuous time series of this length.

2. Methods

2.1. Study site and hydrographic description

The GR mooring (owned and maintained by the National Data Buoy Center as NDBC-41008; http://www.ndbc.noaa.gov/station_page.php?station=41008) with a NOAA $MAPCO_2$ system is located at the ~20 m isobath, ~74 km southeast of Savannah, Georgia and ~40 km east of Altamaha River estuary and coastal marshes around Sapelo Island and the Duplin River, along the Georgia coast (31.400°N, −80.868°W; Fig. 1). The GR mooring is located at a previously defined hydrographic boundary of the inner and middle shelf regions of the U.S. SAB (Pomeroy et al., 2000), loosely based on the location of lower saline waters entering the SAB from coastal freshwater sources and Gulf Stream (GS) influences. The SAB is the coastal margin from Cape Hatteras (North Carolina) to Cape Canaveral (Florida). GS intrusions on the shallow inner shelf occur in only ~5% of all reported surface intrusions in the SAB (Castelao, 2011). By the time that upwelled waters from off the shelf reach the inner shelf they have warmed, making them difficult to detect through temperature analysis (Yoder et al., 1985). This ocean margin is also influenced by 10 rivers that empty into the SAB via marsh-dominated estuaries (Fig. 1). Historically, river discharge is at a maximum from December through April with a water residence time on the shelf of one to three months, which is partially dependent on regional river stream flow volume (Menzel, 1993). The Altamaha River and its watershed are the largest in the region, with its delivery of inorganic nutrients linked to eutrophication and increased primary production in coastal marshes and its estuary (Sheldon and Burd, 2013). We assume that the Altamaha River represents the general seasonality and biogeochemical characteristics of other rivers in the region, and likely has the greatest influence on the GR mooring of all the regional rivers. There is a southward flowing coastal current (salinity < 34) that is typically held shoreward of the ~20 m isobath (Fig. 1) and entrains the lower salinity waters (residence time of up to three weeks) coming from the rivers (Menzel, 1993). Seaward of the ~20 m isobath oceanic water influenced by the GS flows north, and then closer to the self break the GS itself also flows north, thus creating a complex hydrographic shelf region (Pomeroy et al., 2000, and reference therein). During wet periods (December to May, peaking in the late winter/early spring) when river stream flow is increased, the coastal low salinity frontal zone may extend out beyond the ~20 m isobath; conversely, when river stream flow is decreased the low salinity region is greatly reduced and held closer to the coast landward of the ~20 m isobath (Blanton and Atkinson, 1983). The SAB has a relatively weak spring bloom, peaking

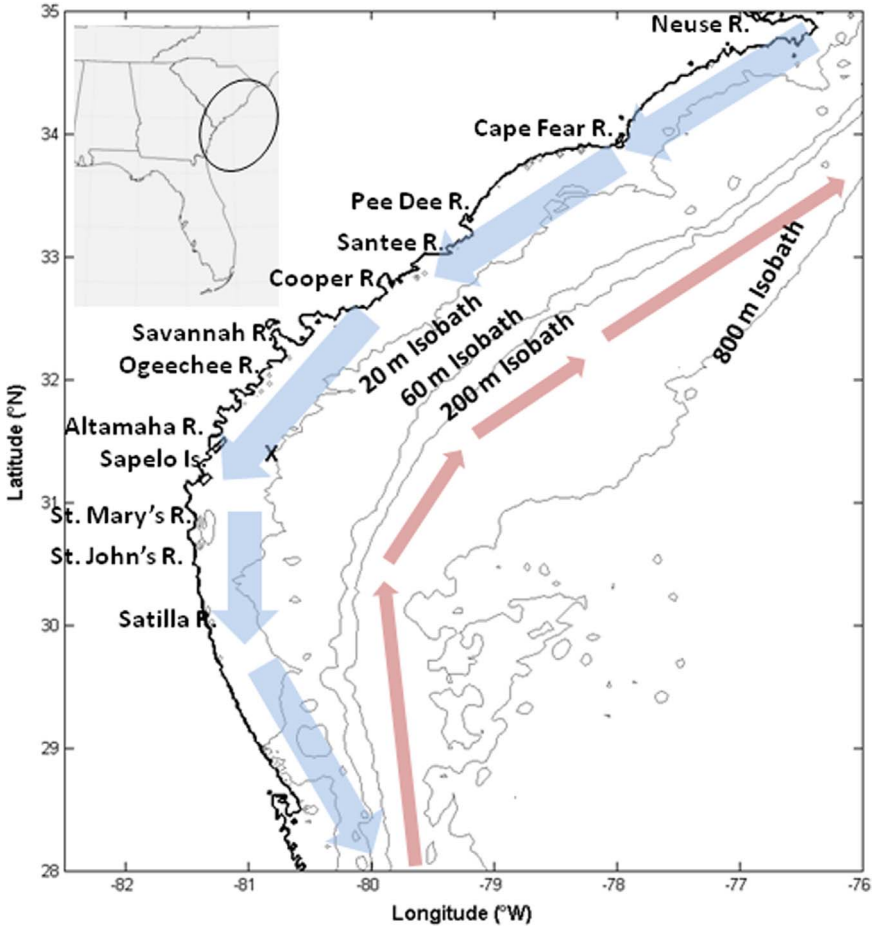

Fig. 1. Map of the SAB showing the location of the GR mooring, the major rivers in the region, and Sapelo Island at the mouth of the Altamaha River. The "X" marks the GR mooring at ~18 m. The wide blue arrows show the general location and directional flow of the low salinity counter current. The northward flowing mean position of the Gulf Stream core are the thin red arrows (see Castelao, 2014). (For interpretation of the references to color in this figure legend, the reader is referred to the web version of this article.)

April through July, as well as small patchy blooms sporadically timed throughout the year (Castelao and He, 2013). The location of the GR mooring allows us to examine terrestrial influences on the CO_2 signal on this ocean margin.

2.2. Compilation of pCO_{2w} observations from cruises

The majority of the cruises that passed close to the GR mooring were not specifically designed for internal consistency measurements of inorganic carbon system parameters, rather they represent years of seasonal cruises that repeated the same transects and stations. A total of 24 cruises were used in this work and are summarized in the Supporting Information Table 1S with more detailed focus on two cruises in 2011 (October) and the July 2015 East Coast Ocean Acidification (ECOA) cruise as specific examples of the ground-truthing exercises carried out at the GR mooring (See Supporting Information). Most cruises collect continuous observations (2–3 min intervals) of surface pCO_2 (dry mole fraction of CO_2 converted to pCO_2 with the accompanying necessary variables (Jiang et al., 2008b)) as well as discrete water samples for DIC and TA, which are used to calculate pCO_2 via the Matlab version of CO2SYS (Lewis and Wallace, 1998; Van Heuven et al., 2009).

DIC and TA samples were collected and analyzed following standard methods with measurement precision of ± 0.1% (Huang et al., 2012) and accuracy of ± 2 μmol kg^{-1}, tested with Dickson Certified Reference Materials (CRM). DIC and TA from bottle samples are used to calculate pCO_{2w}. We use the equilibrium constants of Mehrbach et al. (1973) refit by Dickson and Millero (1987) and boron constants from Lee et al. (2010), which give the closest match to mooring pCO_{2w}. DIC samples have also been collected and measured in the Altamaha River at Doctortown, GA (USGS station 02226000) above the head of the tide from November 2000 through the present using the same methods as GR mooring bottle samples. These samples are used to assess the potential for terrestrial sources of DIC to the region represented by the GR mooring.

There were various underway pCO_{2w} analyzers used during the cruises included over the almost 10 years of field campaigns described in this study, however, the general design and system uncertainty are all ± 2 μatm, with calibrations using gas standards at set time intervals of several hours, similar to the MAPCO$_2$ system (Jiang et al., 2008b; Pierrot et al., 2009). When comparing the various pCO_{2w} values, we align the underway and bottle samples to the closest mooring observation, which typically occur every three hours starting at 00:17 UTC, therefore, the closest temporal sample, for either method, is never more than an hour and a half different. Statistical assessment of internal consistency between methods is done following similar methods employed in previous works, such as assessment of linear correlations (r-value), residual values (mean, standard deviation, and median of the difference between the observed value and the predicted value of the linear model), bias (a source of error due to predictor variables), and root mean square errors (RMSE; a measure of the standard deviation between the predicted and observed values of the linear relationship) (Patsavas et al., 2015; Ribas-Ribas et al., 2014). The residual values, RMSE, and bias are all measures of deviations of predicted values of the linear fit, while any one of these estimations of deviations are likely sufficient, since this is a highly variable coastal

margin reporting various estimations creates a strict criteria for agreement. We also assess the potential for surface layer and spatial heterogeneity using SSS and SST differences (ΔSSS and ΔSST, respectively) between the methods. Finally, we explore the potential sources of uncertainty in internal consistency using adjustments made to measured values in CO2SYS.

2.3. Time series observations and data processing

The MAPCO$_2$ system, described in detail in Sutton et al. (2014), has been measuring xCO$_2$ (the partially dry mole fraction of CO$_2$) referenced to water (xCO$_{2w}$; at ~0.6 m depth) and air (xCO$_{2a}$) above the sea surface (~1.5 m), from July 2006 to October 2014 at a sampling interval of three hours. From the same mooring we also have observations of sea surface temperature (SST), sea surface salinity (SSS), other standard MAPCO$_2$ system variables (e.g., atmospheric pressure, and the water vapor pressure to calculate the partial pressure at 100% humidity), and wind speed from NDBC instrumentation. The anemometer is at ~5 m above sea level; therefore wind speed observations for FCO$_2$ are adjusted to 10 m (Jiang et al., 2008b). Wind speed does not consider gust speed, but rather is an hourly average of the second moment (reported by NDBC). The MAPCO$_2$ system is calibrated with standard gasses prior to deployment, has an onboard standard that runs during each measurement cycle, and is also calibrated post deployment, with any necessary corrections applied prior to release of finalized observations (Sutton et al., 2014). pCO$_{2w}$ was calculated following that described in Sutton et al. (2014). We applied quality control/quality assessment checks and gap-filling techniques, which are presented in the Supporting Information. Gap-filled values are not used for internal consistency analyses.

To determine possible attributing factors to pCO$_{2w}$ variability, besides SST and SSS (thermodynamics), we also analyze a time series of Altamaha River stream flow at Doctortown, GA from 2006 through 2014 (data from: http://gce-lter.marsci.uga.edu/portal/usgs_doctortown/historic/data/index.xml). This site is a USGS hydrological monitoring site above the head of the tide (zero salinity), and accounts for approximately 98.5% of the discharge in the Altamaha River watershed (Sheldon and Burd, 2013). The 15 min observations are summed to daily values to show the amount of water flowing through the watershed region and into the estuaries. We assume that while there are complex current patterns that will affect the trajectory of water movement, DIC inputs to the SAB from terrestrial sources (aforementioned DIC samples from the USGS site) in the region could be generally represented by Altamaha watershed DIC.

2.4. Thermal and non-thermal pCO_{2w} calculations

To determine the relative importance of the competing effects of non-thermal and thermal influences on changes in pCO$_{2w}$ (seasonal cycle), we calculate two operationally defined fractions of pCO$_{2w}$ using the decomposition by Takahashi et al. (2002). Eq. (1) defines non-thermal pCO$_{2w}$ (pCO$_{2nt}$), which is normalized to a time series mean SST. Deviations from pCO$_{2nt}$ imply that non-thermal conditions perturb pCO$_{2w}$. Eq. (2) defines mean pCO$_{2w}$ adjusted to mean SST (pCO$_{2t}$), where perturbations of pCO$_2$ indicate that thermal effects impact pCO$_{2w}$:

$$(p\mathrm{CO}_2 \text{ at } \mathrm{SST}_{\mathrm{mean}}) = p\mathrm{CO}_{2\mathrm{nt}} = p\mathrm{CO}_{2\mathrm{w}} \times \exp(0.0412 \times (\mathrm{SST}_{\mathrm{mean}} - \mathrm{SST})) \quad (1)$$

$$(p\mathrm{CO}_2 \text{ at SST}) = p\mathrm{CO}_{2\mathrm{t}} = p\mathrm{CO}_{2\mathrm{mean}} \times \exp(0.0412 \times (\mathrm{SST} - \mathrm{SST}_{\mathrm{mean}})) \quad (2)$$

where pCO$_{2w}$ is the observed value, pCO$_{2mean}$ is the time series mean pCO$_{2w}$, SST$_{mean}$ is the time series mean SST, and SST is the observed value accompanying the pCO$_{2w}$ measurement. The mean values used in these equations are reported in Section 4.1. The value of the exponent (4.12%) is derived for this specific data set over the SST and SSS range of measured DIC and TA oceanic and near-shore end members following the method of Takahashi et al. (1993) and is within 1 µatm of the Takahashi value of 4.23%. The operationally defined fractions can only distinguish seasonal thermal from non-thermal effects (net biological activity including changes in alkalinity, advection, and air-sea exchange), yet these fractions allow us to distinguish periods when each fraction may be the dominant driver of overall pCO$_{2w}$ variability.

2.5. Air-sea CO_2 flux and gas transfer parameterizations

FCO$_2$ is calculated for the time series using the wind speed parameterization with a recently refit Schmidt number normalized to 660 for a rough surface (Wanninkhof, 2014). The method assumes a dependency on the gas transfer velocity (k) derived from wind speed at 10 m above the sea surface (k_{u10}), the solubility of CO$_2$ in sea water (s) as a function of SST and SSS, and the air-sea pCO$_2$ difference (ΔpCO$_2$):

$$F\mathrm{CO}_2 = k \times s \times \Delta p\mathrm{CO}_2 \quad (3)$$

A negative value for FCO$_2$ represents a flux into the ocean and a positive value is a flux from the ocean into the atmosphere.

There are numerous parameterizations for characterizing k_{u10}. This work does not seek to review all options, we present two representative parameterizations one with a cubic wind speed dependence and non-zero intercept under no/low winds (McGillis et al., 2001) (MG01) and a polynomial of gas transfer with wind (Wanninkhof et al., 2009) (W09) to encompass a range due to differences in the bulk parameterization equations. The equations used in this work are:

$$\mathrm{MG01}: k = 3.3 + 0.026\mathrm{U}_{10}^3 \times (Sc \div 660)^{-1/2} \quad (4)$$

$$\mathrm{W09}: k = 3.0 + 0.1\mathrm{U}_{10} + 0.064\mathrm{U}_{10}^2 + 0.011\mathrm{U}_{10}^3 \times (Sc \div 660)^{-1/2} \quad (5)$$

where U_{10} (m s^{-1}) is the wind speed at 10 m above sea level, and Sc is the Schmidt number (normalized to 660). The gas transfer velocity parameterization for the MG01 estimate is thought to encompass the effects of white caps at higher wind speeds. The W09 estimate is a hybrid model developed to encompass other forces that affect turbulence in the surface. It should also be noted that the W09 hybrid model is similar from a quadratic model with a zero intercept for moderate winds $3 < U_{10} < 15$ m s^{-1} ($k = 0.24\ U_{10}^2$), which is commonly used in the literature (Wanninkhof et al., 2009). The most recent update to the gas transfer velocity ($k = 0.251\ U_{10}^2$) also has a zero intercept, and is also not likely to represent the gas transfer well at the GR mooring due to non-wind effects as low winds impacting turbulence and thus k (Wanninkhof, 2014). Uncertainties in FCO$_2$ due to gap-filled pCO$_{2w}$ observations are addressed in the Supporting Information section S3. Annual FCO$_2$ is determined from the sum of the three hour measurements for each day and the daily standard deviations are summed to represent a general range in which the annual sum is most likely to fall.

3. Results

3.1. Time series of hydrographic and meteorological variables

pCO$_{2w}$ increases in the warmer months and peaks over the summer (Fig. 2B), whereas pCO$_{2a}$ in the marine boundary layer is higher in the colder months (Fig. 2A). The minimum observed pCO$_{2a}$ is 367 µatm (summer 2006) and the maximum is 427 µatm (winter 2012). pCO$_{2w}$ largely follows a recurring seasonal thermal pattern (pCO$_{2t}$; blue line Fig. 2B, C), though excursions are observed, likely indicating influences by non-thermal processes on pCO$_{2w}$ (pCO$_{2nt}$; pink line in Fig. 2B). The daily mean pCO$_{2w}$ of the time series is 409 ± 73 µatm and ranges from 253 (winter 2010) to 567 µatm (summer 2009). Summer (historically dry season, June through September) mean pCO$_{2w}$ ranges from 420 ± 20 µatm in 2006 to 515 ± 20 µatm in 2010, while the winter-spring

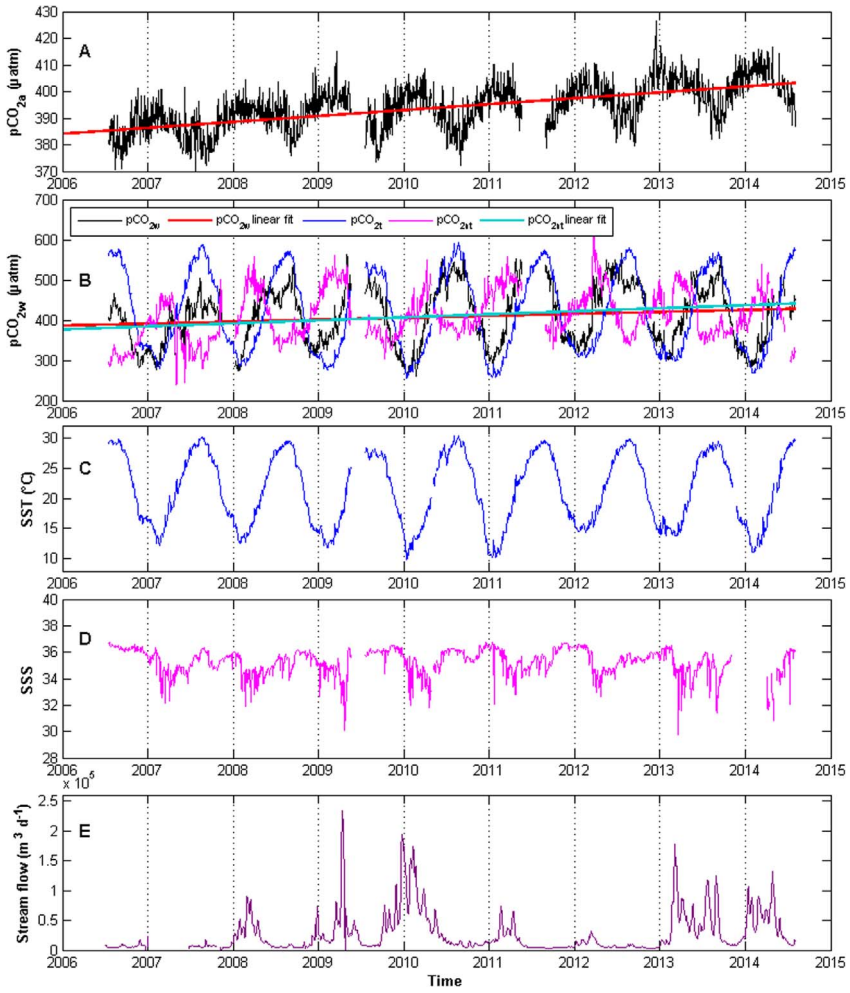

Fig. 2. Time series of variables with slopes of the linear least squares fit. From the top: (A) pCO_{2a} with least squares (red line), (B) pCO_{2w} (black line and red slope line), pCO_{2t} (blue line), and pCO_{2nt} (pink line and light blue slope line) (C) SST, (D) SSS, and (E) Altamaha River stream flow. The trends (slopes) shown are significant at $p < 0.001$ and are significantly different than zero. The values of the trends are also presented in Table 1. Note the difference in scale of pCO_{2a} and pCO_{2w}.

(historically wet season, December through May) pCO_{2w} is lower than the summer (Fig. 2B) with a mean range from 305 ± 37 µatm in 2010 to 368 ± 50 µatm in 2012. pCO_{2t} peaks in the warmer months, following seasonal warming, whereas pCO_{2nt} is highest over the late winter when river stream flow (mixing) is typically increased (Fig. 2B and E). Furthermore, from the late spring to the early winter, pCO_{2nt} decreases when river stream flow typically decreases.

The mean SST is 21.5 ± 5.9 and ranges from 10 to 30 °C (Fig. 2C), and the mean SSS is 35.3 ± 1.0, however, ranges from 29.7, during high volume river stream flow in 2009, to 36.8 at the end of an extended dry period in early winter of 2012 (Fig. 2D). In general, SSS is decreased in the late winter and into the spring when Altamaha River stream flow is increased. Mean U_{10} is 6.0 ± 3.0 m s^{-1} and ranges from < 1–21 m s^{-1}; with the maximum occurring during Hurricane Andrea in 2007. Daily Altamaha River stream flow ranges from approximately 616 m^3 d^{-1} in the dry season (during a drought period) to 233,747 m^3 d^{-1} during a high precipitation event in spring of 2009 (Fig. 2E). Typically, river stream flow into the SAB is increased in the winter cool periods compared to the summer warm periods (Fig. 2E). While there is a large gap in river stream flow data in 2007, it is known to be during a synoptic scale dry period (Sheldon and Alber, 2013). DIC in the Altamaha River is decreased in the winter during increased river stream flow periods, while is it increased during decreased river stream flow (Fig. 3A).

Over the ~8.5 years of the time series we fit linear least squares regressions, which minimizes the effects of high variability in data sets, to determine if there are overall increases or decreases in daily mean values for all variables. Using a daily mean value also helps to eliminate the effects of noise by essentially smoothing the daily variations. The linear fit (slope), which is calculated from mid-July 2006 (beginning of the time series to the end of June 2014), is considered statistically significant if the correlation coefficient (p-value) is < 0.05 and the 95% confidence interval (CI) does not overlap with zero. There are increases over the time series in pCO_{2a} and pCO_{2w} of 2.2 ± 0.2 and 4.9 ± 2.4 µatm y^{-1}, respectively, as well as an increase of 7.6 ± 1.9 µatm y^{-1} in pCO_{2nt} (Fig. 2A and B; Table 1). A linear least squares analysis will be influenced by the start and end points of the data analyzed, however, we attempt to minimize this effect by analyzing full annual cycles starting from the beginning of the time series. We do not consider shorter periods of time over the time series (i.e., multiannual droughts or wet periods) that could be influenced by large episodic variability, which could influence trends. There were no statistically significant changes for, pCO_{2t}, SST, SSS, or Altamaha River stream flow over the time series (Table 1 and Fig. 2B–E, respectively). There is a 15 ± 10 µmol kg^{-1} DIC increase (calculated based on bi-weekly sampling, on average) from January 2001 through January 2014. The DIC observations collected over the time period of the GR time series (July 2006 through July 2014) are too few to give a meaningful result, therefore we extended this data analysis to include all our available DIC observations. The 95% CI of ± 10 µmol kg^{-1} DIC is almost the same as the estimated increase, likely due a combination of high seasonal variability, as well as data gaps and sampling bias, which was less frequent from 2013 through 2014.

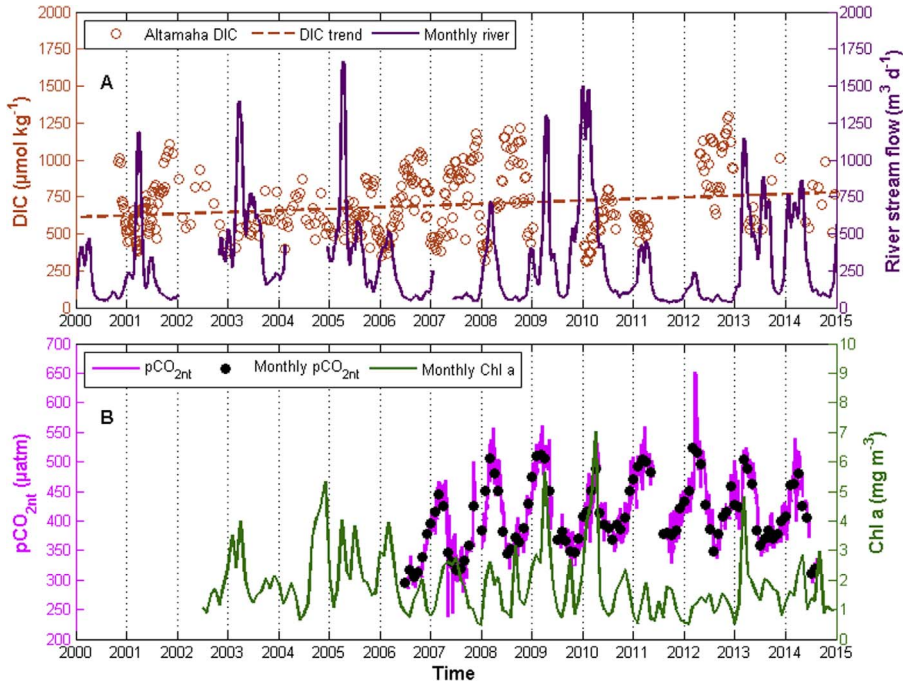

Fig. 3. This figure shows some of the different biogeochemical components of the pCO_{2nt} (plotted in panel B): in panel (A) mixing, represented by Altamaha River stream flow (smoothed over a 30 day period) and biological contributions from DIC (at the Doctortown, GA USGS site) in the watershed. In panel (B) monthly mean Chl *a* as a proxy for local biological consumption of CO_2 and pCO_{2nt} (daily mean time series and monthly means).

In Fig. 3B we include chlorophyll *a* (Chl *a*; 4 km monthly means centered on the Latitude-Longitude of the GR mooring from the NASA Giovanni server: http://gdata1.sci.gsfc.nasa.gov/daac-bin/G3/gui.cgi?instance_id=ocean_month) and re-plot pCO_{2nt} to clearly illustrate the behavior of pCO_{2nt} with respect to Chl *a*. There was no significant trend in monthly Chl *a* over the course of the GR mooring time series, nor from the beginning of NASA time series. The highest Chl *a* events occur in the spring of the wettest years (2009, 2010, and 2013; Fig. 3B). The average Chl *a* for the site is 1.73 ± 1.09 mg m^{-3}, with a median value of 1.48 mg m^{-3} and a range of 0.48 (January 2012) to 7.04 mg m^{-3} (April 2010).

3.2. FCO_2 time series and annual net sums of FCO_2

FCO_2 is positive (degassing) over the warmer months, and negative in the cooler months following the seasonal ΔpCO_2 cycle (Fig. 4). The mean U_{10} seasonal (November-April versus June-October) variation is < 1 m s^{-1}, even though in the summer when U_{10} is slightly decreased, FCO_2 still closely follows ΔpCO_2 (Fig. 4).

ΔpCO_2 becomes more positive over the time series, increasing at a rate of 2.6 ± 2.5 µatm y^{-1} (Fig. 4D and Table 1). The change in FCO_2 from July 2006 through June 2014 is not significant, likely due to the high variability, thus the large 95% CI's (Table 2). Analyzing the trend from the beginning of the time series through the end in October 2014, however, results in an increase of 51 ± 25 mmol m^{-2} y^{-1} to 70 ± 34 mmol m^{-2} y^{-1} for the W09 and MG01 wind speed parameterizations, respectively. The two k_{u10} parameterizations used in this work have similar seasonal patterns (Fig. 4A & B), however, annual estimates using the different parameterizations do not always agree on whether the site is a net source or sink for atmospheric CO_2 (Fig. 5). The difference in source/sink estimate is because while both *k*-values are always positive and ΔpCO_2 is the same in both cases (but may be negative), the difference in the annual FCO_2 sign must come from high wind periods where the two *k*-parameterizations diverge. The difference between the annual net FCO_2 estimates can be up to 0.60 mol m^{-2} y^{-1} in 2008 (Table 2). The error bars in Fig. 5 represent the uncertainty in FCO_2 using daily mean values to determine the air-sea exchange, and are a sum of the standard deviations of means for each day with measurements (the number of days with measurements is in the parentheses in Table 2). We do not have observations for every day over the ~8.5 years; the sums represent a total for days with observations including days that are gap-filled.

3.3. Internal consistency between the mooring, underway, and DIC-TA calculated pCO_{2w}

All internal consistency correlation results and residual values are summarized in Table 3 and Figs. 6 and 7. Fig. 6 depicts the linear correlations of the measurement methods in terms of measured salinity differences and Fig. 7 highlights the correlations in terms of measured SST differences. Over the ~8.5 years of the time series the mooring-bottle and mooring-underway pairs correlate with $r > 0.90$ ($p < 0.001$),

Table 1
Summary of pCO_{2w} internal consistency. GR Mooring observations are from 0.6 m, whereas underway are from 2.5 to 4 m, and bottle samples from 0 to 4 m. All units are µatm and in each instance the residual value is the first method minus the second method. The root mean squared error (RMSE) gives a statistical result for the error in the correlation model. The values for the best fit slope and intercept for the linear equation. "Bottle" pCO_{2w} is calculated from DIC and TA.

Pairing	Correlation statistics	Mean, Stdev, and median residual	Best fit slope & intercept	Mean Bias
Mooring-Underway	r = 0.92; $p <$ 0.001; n = 51; RMSE = 17.6	5.54 ± 32.4, 8.2	0.76, 102	12.3 ± 21.3
Mooring-Bottle	r = 0.91; $p <$ 0.001; n = 57; RMSE = 24.6	24.4 ± 29.0, 25.0	0.79, 70.4	24.6 ± 30.7
Underway-Bottle	r = 0.84; $p <$ 0.001; n = 41; RMSE = 28.3	24.8 ± 29.2, 12.2	0.76, 80.7	21.2 ± 35.5

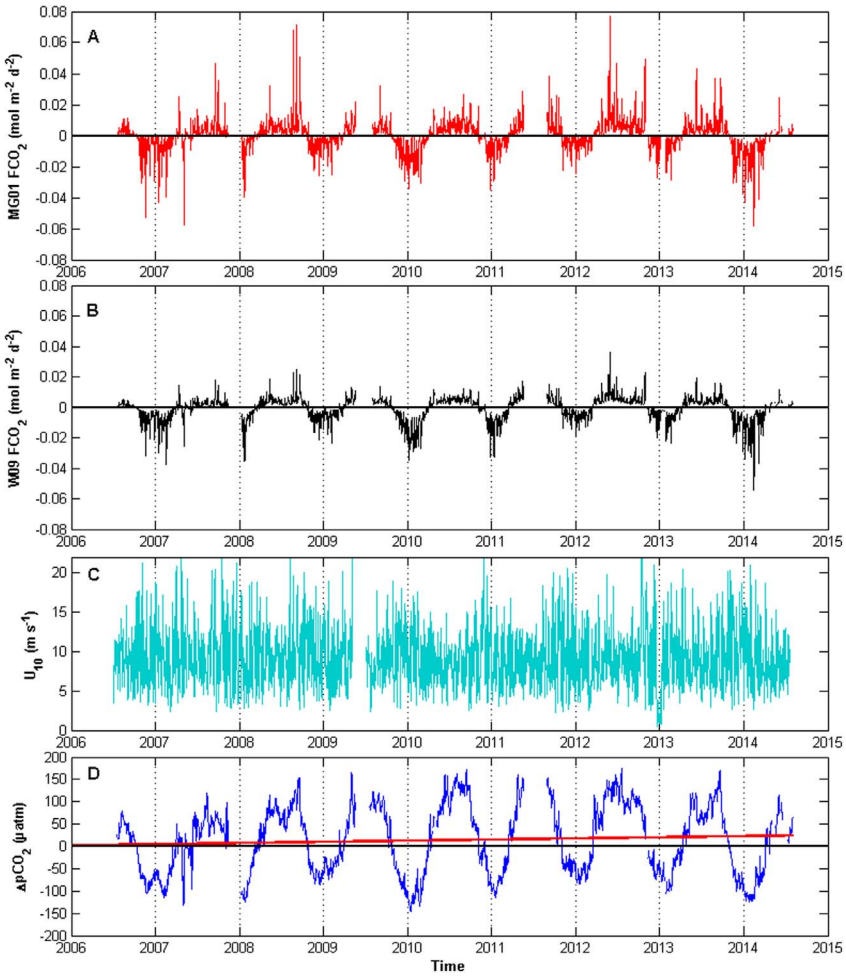

Fig. 4. Time series of (A) the MG01 FCO_2 and (B) W09 FCO_2 estimates; (C) U_{10}; and (D) the air-sea pCO_2 difference (ΔpCO_2). The red line in panel D is the linear least squares best fit line that indicate a statistically significant increase. Negative values indicate a flux into the sea surface and positive values indicate a flux into the atmosphere.

however, the bottle-underway pair only correlate to $r = 0.84$ ($p < 0.001$; Table 1). The bias results for each method suggest that both underway and bottle pCO_{2w} underestimate (best fit slope in Fig. 6A and C is less than 1) the mooring value and that underway pCO_{2w} is less biased (mean bias of 12.3 ± 21.3 µatm; Table 3) than bottle-calculated pCO_{2w}. The difference between the mean residual and median residual for the individual methods, as well as the high standard deviations (Table 3), suggests that outliers influence the general relationships, and further examination of the sources of these differences must be assessed.

Since this is a coastal region influenced by freshwater sources, likely with high spatial heterogeneity, we examine method discrepancies in pCO_{2w} using SSS (freshwater influence) and spatial distance from the mooring (Fig. 6). We initially assume that 1) the distance between where the bottle sample is taken and the closest temporal underway observation (no more than 2 min) is recorded is negligible; and 2) a salinity difference could be due to sensor uncertainty and/or error, as well as vertical differences in the water column caused by stratification (different sampling depths) or horizontal differences caused by advection. Both SSS differences and distance can be a factor, yet there is no one clear pattern (Fig. 6). For example, bottle samples taken at the mooring can have 0 to < 0.6 SSS unit difference with 20–70 µatm pCO_{2w} discrepancies, while samples taken at a greater distance, with ~2 SSS unit differences, can have only ~10 µatm pCO_{2w} discrepancies (Fig. 6D). There are similar results for underway observations (Fig. 6B). Specifically for the difference between mooring and bottle pCO_{2w} there is a weak dependence explained by the SSS measured by the mooring ($r^2 = 0.22$; $p < 0.001$; $n = 57$): at lower SSS mooring pCO_{2w} is greater than bottle-calculated pCO_{2w} (Fig. 6F). The spatial

Table 2
Linear least squares fit results for time series of variables with statistically significant results. In the least squares fit equation "t" is the unit of time (per day). The units of annual change are µatm y^{-1} for CO_2 fractions, mmol m^{-2} y^{-1} for FCO_2, and µmol kg^{-1} for DIC. *These results are for July 2006 through October 2014, the linear model is not significant July 2006 through July 2014.

	Regression	95% CI	Least squares fit	Annual change
pCO_{2a}	$r^2 = 0.37$; $p < 0.001$; $n = 2636$	5.8 to 6.4 × 10^{-3}	$pCO_{2a} = (6.1 \times 10^{-3}) \times t + 384.1$	2.2 ± 0.2
pCO_{2w}	$r^2 = 0.02$; $p < 0.001$; $n = 2636$	1.0 to 1.7 × 10^{-2}	$pCO_{2w} = (1.3 \times 10^{-2}) \times t + 386.0$	4.9 ± 2.4
pCO_{2nt}	$r^2 = 0.08$; $p < 0.001$; $n = 2612$	1.8 to 2.3 × 10^{-2}	$pCO_{2nt} = (1.9 \times 10^{-3}) \times t + 376.3$	7.6 ± 1.9
ΔpCO_2	$r^2 = 0.006$; $p < 0.001$; $n = 2636$	5.3 to 12 × 10^{-3}	$\Delta pCO_2 = (8.5 \times 10^{-3}) \times t + 0.39$	3.1 ± 2.4
MG01 FCO_2*	$r^2 = 0.03$; $p < 0.001$; $n = 2486$	1.5 to 2.4 × 10^{-6}	$FCO_2 = (1.9 \times 10^{-6}) \times t - (2.6 \times 10^{-3})$	70 ± 34
W09 FCO_2*	$r^2 = 0.03$; $p < 0.001$; $n = 2486$	1.1 to 1.7 × 10^{-6}	$FCO_2 = (1.4 \times 10^{-6}) \times t - (1.9 \times 10^{-3})$	51 ± 25
DIC	$r^2 = 0.05$; $p < 0.001$; $n = 455$	0.02 to 0.005	DIC = 0.04 × t + 611	15 ± 16

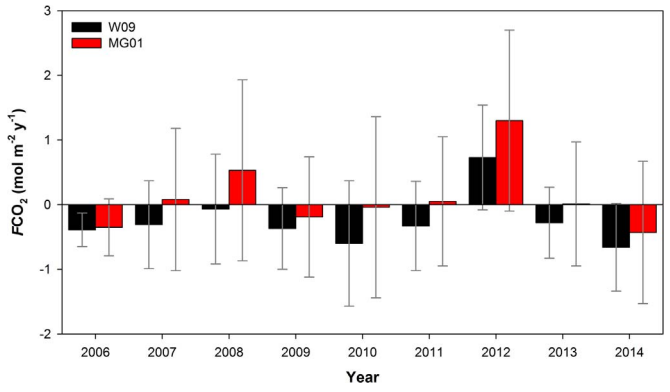

Fig. 5. Annual FCO_2 using the two gas transfer parameterizations. The error bars are the sum of the daily standard deviations for W09 and MG01. Given considerable data loss in 2014, which was gap filled at a daily frequency, thus we do not have daily standard deviations for the whole year as we do for other years. Therefore, the error for year 2014 is the mean error from all other years. Larger data gaps occurred in 2007, 2009, 2011, 2013, and 2014 (end of deployment not finalized); see Table 3 for the number of missing days.

Table 3
Annual net FCO_2 at the GR mooring and the sum of the daily standard deviations. The number of days for which there are missing observations after interpolation and gap-filling is in parenthesis following the year in the first column. W09 and MG01 are the two estimates for FCO_2, respectively. Since the time series begins in July of 2006, we only have data for the second half of the year, and because the deployment for the mooring ends in October of 2014, observations are not yet available for use for the end of 2014 through the present. Units are in mol m^{-2}.

Year	W09 (mol m^{-2} y^{-1})	MG01 (mol m^{-2} y^{-1})	MG01-W09
2006 (198)[a]	−0.39 ± 0.26	−0.35 ± 0.44	0.02
2007 (49)	−0.31 ± 0.68	0.08 ± 1.1	0.39
2008 (9)	−0.07 ± 0.85	0.53 ± 1.4	0.60
2009 (73)	−0.37 ± 0.63	−0.19 ± 0.93	0.18
2010 (13)	−0.60 ± 0.97	−0.04 ± 1.4	0.56
2011 (100)	−0.33 ± 0.69	0.05 ± 1.0	0.38
2012 (10)	0.73 ± 0.81	1.3 ± 1.4	0.57
2013 (64)	−0.28 ± 0.55	0.01 ± 0.96	0.29
2014 (53)[b]	−0.66 ± 0.68	−0.43 ± 1.1	0.23

[a] The time series began in July of 2006.
[b] 53 days are missing from the time series through the end of the deployment, which was October 24, 2014; however, the total missing for the 2014 calendar year is 122.

distribution of SSS around the mooring is discussed in section S4 of Supporting Information (Fig. S1).

Differences in SST between the bottle samples, the mooring system, and the underway systems may also contribute to discrepancies (Fig. 7A). Adjusting calculated pCO_{2w} and underway pCO_{2w} to mooring SST (as well as adjusting using both SST and SSS) did not improve the strength of correlations (Fig. 2S). Similar to pCO_{2w} discrepancies due to SSS, even smaller SST differences can have associated higher pCO_{2w} discrepancies between methods (Fig. 7B), which are not always caused by thermodynamic differences (See Supporting Information section S4). Sources of pCO_{2w} discrepancies could include measurement error (e.g., system calibrations, contamination, improper storage), measurement uncertainty due to problems with the DIC and TA methods (e.g., measurement precision or inclusion of organic alkalinity; Fig. 3S), and/or spatial heterogeneity, and are summarized below and discussed in the Supporting Information section S4.

Using two examples of cruises we illustrate when validation efforts have provided good agreement between all methods and when they did not, in an attempt to improve future sensor validation efforts in the SAB and other moorings. The first example, one of only a few less successful cruises, in Fig. 8A, illustrates the spatial track of the October 2011 cruise. During this diel period the pCO_{2w} at the mooring ranged from 420.7 to 444.9 µatm, with the minimum occurring at approximately 22:00 UTC and the maximum at 15:00 UTC (Fig. 8B). Bottle samples ranged from 383.3 to 409.2 µatm (Fig. 8B). The mean residual between mooring and underway observations is 2.5 ± 20 µatm, with a median of 4.8 µatm (n = 51) and between mooring and bottle the mean is −36 ± 11 µatm with a median of −37 µatm (n = 57). The spatial-temporal differences observed during this cruise represent distance from the mooring (up to ~0.9 km) as well as changes in pCO_{2w} not captured by the three hour frequency of mooring measurements (Fig. 8A). It is also important to note the vertical difference in the water column, which may cause the greater pCO_{2w} difference between the bottle values at 4 m and those from the underway (2.5 m) and the mooring (0.6 m). In the second, more successful example, in Fig. 9A, the average mooring pCO_{2w} during ECOA July 2015 is 446.4 ± 0.4 µatm and the average bottle calculated value is 446.7 ± 3.8 µatm (Fig. 9B), which are not statistically different. The mean and median residual mooring-underway are −4.9 ± 5.2 µatm and the mooring-bottle mean and median residual are < 0.1 ± 3.8 µatm and 1.9 µatm, respectively. Regardless of the spatial difference (up to 1.6 km and ~3 m depth), there is good agreement between the three methods during the ECOA 2015 cruise, which likely indicates spatial homogeneity as opposed to the October 2011 cruise, and will be discussed in more detail below.

4. Discussion

4.1. pCO_{2w} internal consistency and validation

We assess pCO_{2w} internal consistency of mooring, underway, and bottle samples using a combination of correlation results, residual values, and biases (Table 3). At this time we do not offer specific values for allowable agreement since the majority of the cruises were not designed with validation in mind, rather use this discussion not only to address the positive outcomes of internal consistency, but also challenges and how they can be addressed and improved in future work. In general, internal consistency is comparable among the three methods, as well as to other studies, however, Figs. 6–8 also illustrate the often problematic spatio-temporal heterogeneity of the system. First, we find that the strongest agreement with the lowest bias is between the mooring-underway pair (Table 3). Using two independent underway pCO_2 systems on the same cruise, similar correlation results (r = 0.96) were obtained by a previous study (Ribas-Ribas et al., 2014). Our result may be slightly weaker than previously published correlations due to high spatial heterogeneity, which would not be expected when comparing two different systems on the same vessel as opposed to locations up to 2 km apart. Second, our mooring-bottle correlation (r = 0.91) is similar to the mooring-underway (r = 0.92), however, the RMSE greater for the mooring-bottle pairing (24.6 µatm) than the mooring-underway pairing (17.6 µatm), suggesting that while the mooring-bottle method is in good agreement, there is an overall potential for differences in these methods of an order of magnitude greater than system uncertainties (Schar et al., 2010; Sutton et al., 2014). Previous work has included Monte Carlo re-sampling to estimate an allowable range of uncertainty (Ribas-Ribas et al., 2014), however, this is not a practical approach for the present work since our sample size is limited and could bias results. In general, internal consistency with respect to the mooring is good and results provide knowledge needed for future work (discussed below).

We identify several potential sources of pCO_{2w} discrepancies within the data set, which are being used to improve present and future validation efforts at the GR mooring. Detailed analyses of the sources of differences among methods are discussed in the Supporting Information section S4, in summary:

- Poor analytical and storage methods for the DIC-TA pairing could

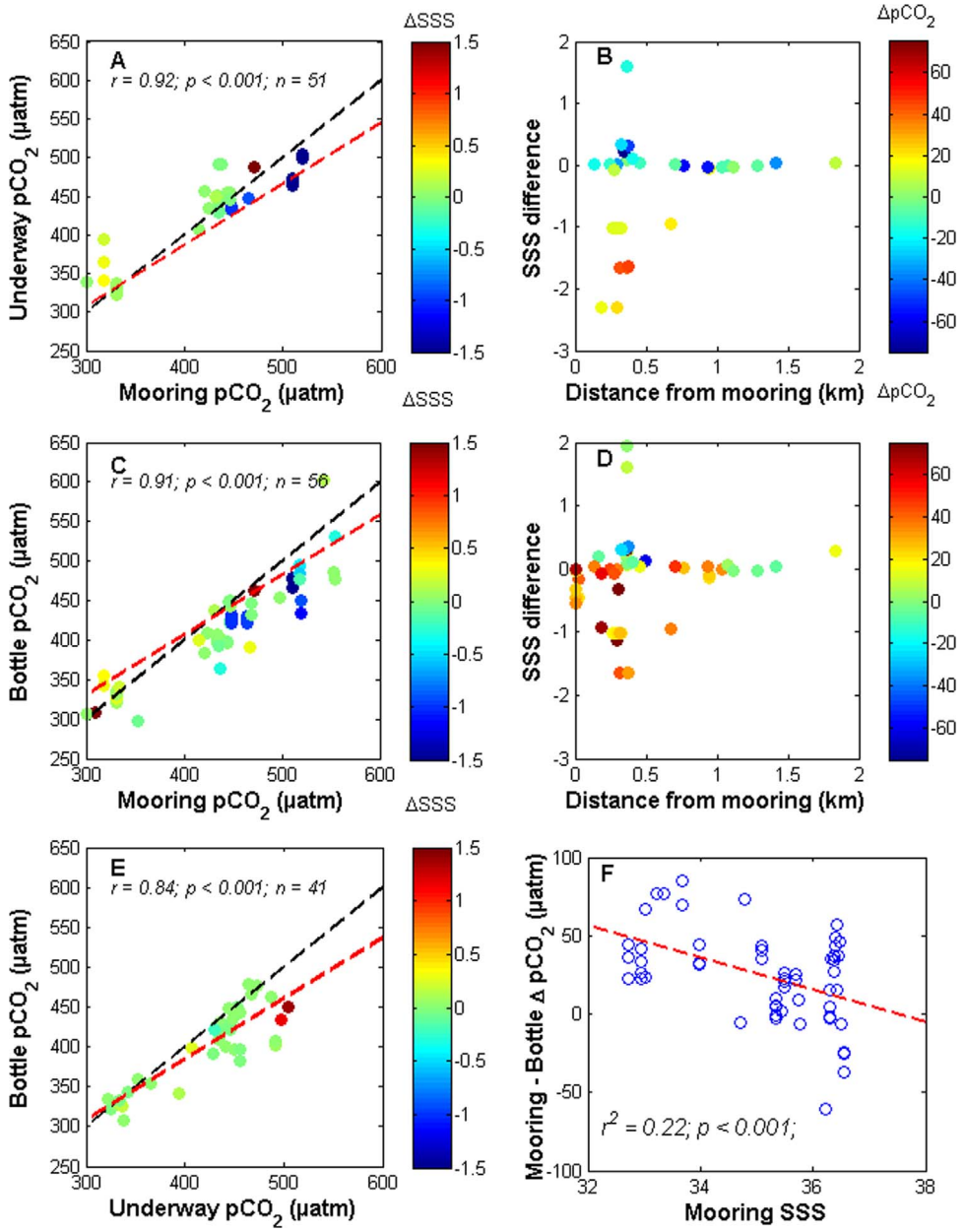

Fig. 6. Internal consistency correlations from the three different pCO_{2w} observation methods using SSS and distance from the mooring to examine sources of discrepancies. Panels A, C, and E are the results of correlation analyses, and B and D are comparisons of spatial distance and SSS differences between the mooring and the other method. In this graphic ΔpCO_2 is the difference between pCO_{2w} from the x-axis minus pCO_{2w} from the y-axis. Panel F is the pCO_{2w} difference between the mooring and that calculated from DIC-TA of the bottle with respect to the SSS measured at the mooring. The black lines in all panels are the 1:1 lines and the red lines are the best-fit lines (slopes and intercepts are in Table 2).

contribute up to 10% relative mean uncertainty in calculated pCO_{2w}, a value well above internationally accepted ocean acidification monitoring network best practices (Newton et al., 2014). Poor storage could result in increased pCO_{2w} in bottle samples due to respiration, or decreased pCO_{2w} due to degassing.

- Spatio-temporal SSS during the two cruises highlighted (October 2011 and ECOA-2015) only had mooring-underway SSS difference of up to ± 0.2, however, including all cruises the maximum SSS difference was up to ~2.3 (Fig. 6B and D). If for every theoretical 1 unit SSS changes, the TA changes ~50 µmol kg^{-1} (Xue et al., 2016), then the 0.2 or 2.3 unit difference could account for a TA difference ranging from ~10–115 µmol kg^{-1}, respectively. Therefore, potentially affecting the pCO_{2w} value of one method with respect to the other.
- Assuming that sensor differences or environmental differences represented by differing SST could contribute to discrepancies in pCO_{2w} we adjust underway and bottle SST to mooring SST (Eq. (1) of Supporting Information; Takahashi et al., 1993). This adjustment, however, decreases the overall strength of correlation results, though in some individual instances does decrease the discrepancies between methods (Fig. S2). Therefore, environmental or sensor differences could affect some cruise results but in general are not likely the primary source of discrepancies in the present work.
- On a coastal margin influenced by freshwater, SSS spatio-temporal heterogeneity may also be important and indicates if different water masses are sampled. Since SSS only explains up to 87% of TA variability in bottle samples ($p < 0.001$), a portion of TA could be due to organic bases, thus overestimating TA and subsequently underestimating pCO_{2w} (Yang et al., 2015). Decreasing measured TA in this study 10–30 µmol kg^{-1} increased the correlation strength for mooring-bottle (Fig. 3S) as well as reduced the RMSE and residual values. Therefore, organic bases in the TA method, resulting in systematic biases in calculated pCO_{2w}, could skew results on

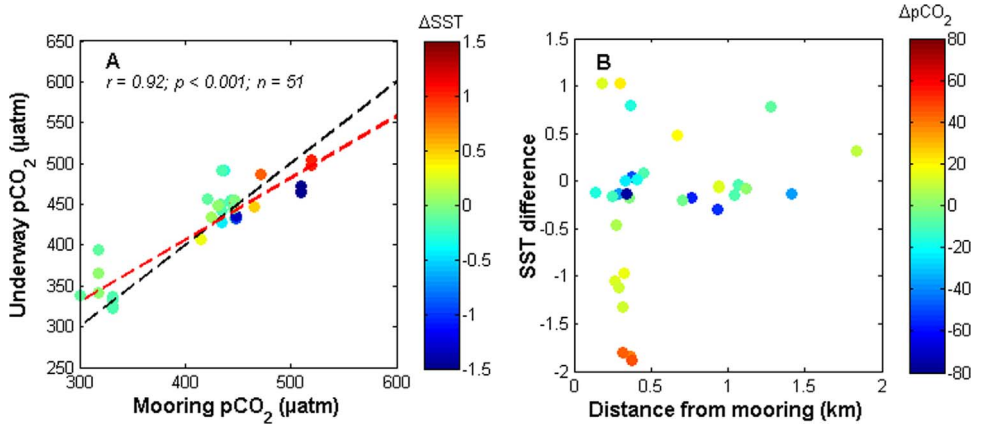

Fig. 7. Internal consistency correlation for results between mooring and underway pCO_{2w} using SST to examine sources of pCO_{2w} discrepancies. Panel A is the result of correlation analysis illustrating the same pCO_{2w} relationship in Fig. 2A, however, with the color bar representing the difference in SST between the mooring and underway observations. Panel B is the comparison of spatial distance and SST differences between the mooring and underway observations. In this graphic ΔpCO_2 is the difference between pCO_{2w} from the x-axis minus pCO_{2w} from the y-axis. The black line is the 1:1 line and the red line is the best fit-line.

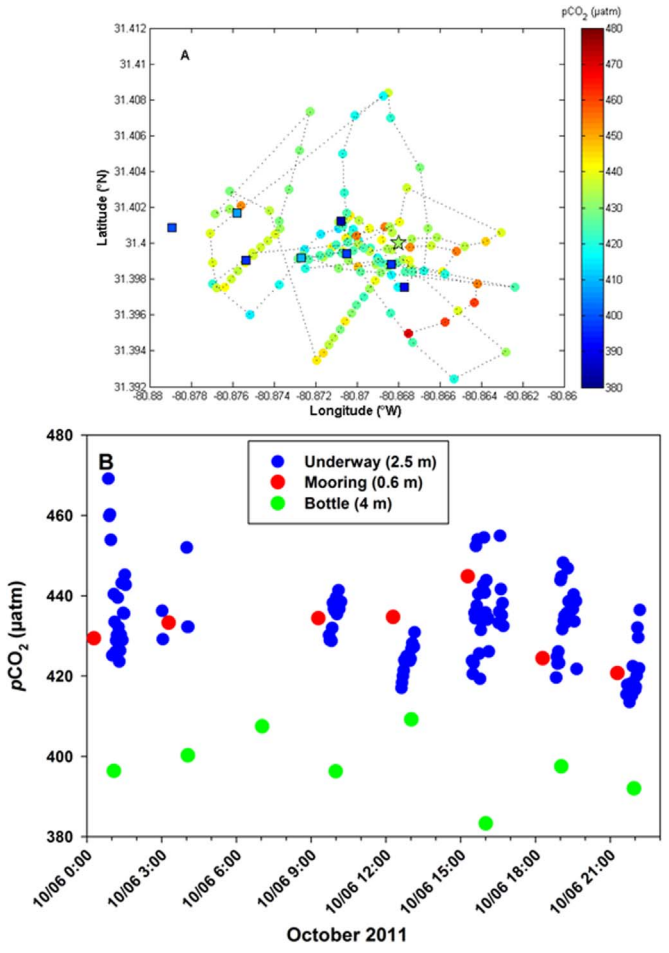

Fig. 8. October 2011 internal consistency of (A) spatial underway pCO_{2w}, bottle-calculated pCO_{2w}, and GR mooring pCO_{2w} and (B) the observations plotted over time. The star in panel A is the mean from the mooring over the time period of the ground-truthing pass and the squares are the bottle samples. The gaps in underway observations in panel B either represent instrument calibration periods (typically on the order of 25 min), when the system was shut down to clean the filters (this region can be highly turbid, especially during wet periods), or are points that were omitted when the ship moved too far from the mooring.

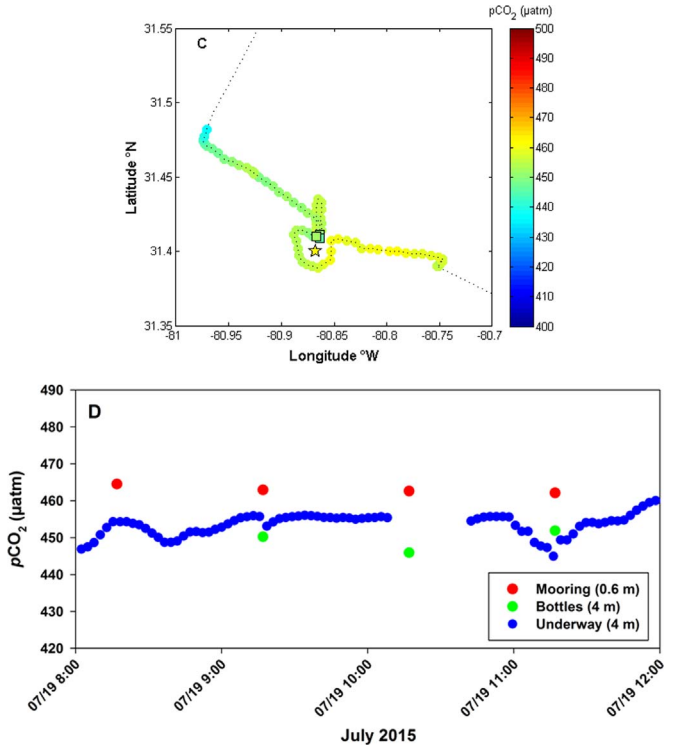

Fig. 9. July 2015 internal consistency of (A) spatial underway pCO_{2w}, bottle-calculated pCO_{2w}, and GR mooring pCO_{2w} and (B) the observations plotted over time. The star in panel A is the mean from the mooring over the time period of the ground-truthing pass and the squares are the bottle samples. The gaps in underway observations either represent instrument calibration periods or were omitted when the ship moved too far from the mooring. Note that the scale of the color bar in panel (A) is different than the scale in panel (A) of Fig. 4. Note the difference in spatial scale between panel A of this figure and panel 4A.

coastal margins. Given this conclusion, future validation efforts could include deeper investigation on the role of organic bases in TA measurements at the GR mooring.

While at this time we do not seek to examine environmental details of every individual cruise for sources of internal discrepancies in calculated pCO_{2w}, we note that these previous validation efforts are an important step in better understanding spatio-temporal CO_2 dynamics at this particular field site. The pCO_{2w} differences observed at this site could also be due to the influence of tidal or temperature fronts (advection of coastal or oceanic water masses) on very small spatial and temporal time scales (Figs. 6–9). Future validation attempts, if they cannot be performed within meters and minutes of the mooring observation, should consider tides and also attempt to

identify any different water masses around the mooring that could influence the results. Spatial differences are more likely to occur using mooring-underway validation, whereas, temporal differences are less likely to be responsible for pCO_{2w} differences given the high temporal frequency of underway observations. Conversely, given that we know the mooring samples at 17 min after the hour, though the observation is integrated over a 6 min equilibration time, temporal differences should be less of an issue if samples are taken at the mooring.

The magnitude of the mooring-bottle results are similar to those determined for a $MAPCO_2$ system in the Hood Canal (Washington, USA), however, in that instance calculated pCO_{2w} was greater than the moored value (−12 ± 30 μatm), and the difference between mooring and underway pCO_{2w} was better (−9 ± 8 μatm) (Schar et al., 2010). Consistent with the aforementioned study we find that there is better agreement between mooring-underway than mooring-bottle using the DIC-TA pairing, which could be due to analytical challenges using calculated pCO_{2w}. A reasonable understanding of the bottle-mooring pair is needed in order to use SSS-derived TA and pCO_{2w} to accurately estimate the rest of the carbonate system variables at the GR mooring (Sutton et al., 2016) in future works. Once we are able to calculate all carbonate system variables, with a good sense of validity through internal consistency, then we can apply biogeochemical and/or more sophisticated physical-biological coupled models in the future to better understand the sources of pCO_{2w} variability on this coastal margin. This initial validation is a first step in showing that reasonable internal consistency has been achieved at this mooring and that GR mooring time series measurements are good quality and can be used to assess pCO_{2w} at this site. Given how measurement methods have changed over the last decade, as OA and carbonate system variable observations have become crucial, this is an important milestone in carbonate system studies. The next step in future time series research is to compare OA monitoring site results from present studies to those conducted prior to the initiation of our present $MAPCO_2$ systems as well as to historic observations.

4.2. Seasonal to interannual pCO_{2w} and FCO_2 variability

Intra-annual pCO_{2w} variation follows a seasonal thermal cycle, with increased partial pressure in the summer compared to the winter. When pCO_{2w} is decomposed, pCO_{2t} and pCO_{2nt} exhibit out-of-phase seasonal harmonics that roughly coincide with SST and river stream flow cycles, respectively (Figs. 2 and 3). The almost identical phases of pCO_{2w} and pCO_{2t} (or SST), as well as the greater seasonal amplitude of pCO_{2t} compared to pCO_{2w}, support a SST-dominated seasonal cycle (Fig. 3B and C). Rather than examining well defined pCO_{2w} seasonal thermal cycles in the SAB, as has recently been done (e.g., Signorini et al., 2013; Xue et al., 2016), we assess the potential contributions to seasonal pCO_{2nt} variability and interannual changes.

pCO_{2nt} variability, which is out of phase with observed pCO_{2w}, reflects the overall influence of non-thermal processes: vertical and/or horizontal mixing (river stream flow), net biological reactions, and air-sea exchange (Xue et al., 2016). GR mooring pCO_{2nt}, which is increased in the winter and early spring with the river discharge, decreases as spring time Chl *a* increases (Fig. 3). The timing of pCO_{2nt} variability strongly suggest that the initial pCO_{2nt} increase is a response to terrestrial CO_2 exported from the Altamaha River (Fig. 3), as a proxy for all freshwater sources to the SAB. Even though riverine DIC concentration decreases (dilution) with increased river stream flow (Fig. 3A), not only would the overall lateral flux out of the watershed be enhanced but, the CO_2 to DIC ratio would increase as well (Jiang et al., 2013) at higher stream flow. Increased river discharge also mobilizes material (OM, CO_2, DIC, and inorganic nutrients) export fluxes from salt marshes via tidal flushing (Cai, 2011), thereby enhancing lateral fluxes across the SAB inner shelf. Consequently, exported OM likely provides a sustainable source for CO_2 via respiration on the shelf (Cai et al., 2003; Jiang et al., 2013, 2010; Pomeroy et al., 2000) possibly even after river stream flow decreases.

Another consequence of increased river discharge in the winter and early spring is an increase in nutrient export from the watershed, estuaries, and marshes (Fig. 3) (Cai et al., 2003; Jiang et al., 2013; Schaefer and Alber, 2007). We suggest that nutrient export is the cause of increased Chl *a*, an indicator of biomass, during the spring and early summer at the GR mooring starting from when spring SST warming begins. As a result in the spring-early summer pCO_{2nt} decreases following the Chl *a* peak as biological production consumes CO_2 (Fig. 3B). Overall pCO_{2w}, however, increases due to warming (pCO_2), leading to degassing and positive FCO_2 (Fig. 4), therefore, pCO_{2nt} continues to decrease in the warm summer months due to the switch from negative to positive FCO_2. Finally, in the fall-winter pCO_{2nt} increases once again due to lateral transport and respiration of OM exported from estuaries earlier in the season, as well as heterotrophy on the shelf (Pomeroy et al., 2000). When SST cools, FCO_2 returns to negative, which also contributes to the pCO_{2nt} increase via atmospheric CO_2 uptake (Figs. 2 and 4). While the aforementioned processes all contribute to overall pCO_{2w} and pCO_{2nt} their relative importance likely varies season-to-season and interannually, as was reported by Xue et al. (2016).

4.3. Sub-decadal CO_2 trends and larger scale implications

pCO_{2w} increases over the time series, though still on a sub-decadal scale, by 5.2 ± 1.4 μatm y^{-1}. The large data loss in 2009 is in the middle of the time series, and therefore does not greatly influence the long-term trend. The pCO_{2w} increase is more than double the pCO_{2a} increase at this coastal site, as well as the rate at the Bermuda Atlantic Time Series (BATS) station (1.7 ± 0.09 μatm y^{-1}) (Bates et al., 2014, 2012) and the global mean pCO_{2a} ~2.0 μatm y^{-1} (Wanninkhof et al., 2013). Such increases in pCO_{2w} have also been noted in the northern South China Sea, which is increasing at a rate slightly higher than that of the atmosphere (Tseng et al., 2007). Also, pCO_{2w} in the North Sea between two summers is increasing at a rate 5–6 times the atmospheric, thus decreasing the net regional sink (Thomas et al., 2007), which could also be the case at the GR mooring and SAB inner shelf. Furthermore, at the GR mooring there is a 7.1 ± 1.9 μatm y^{-1} pCO_{2nt} increase. Consistent with previous studies in the North Atlantic basin (Fay and McKinley, 2013; McKinley et al., 2011), we find that GR mooring pCO_{2w} change over the course of our time series does not reflect an increase in SST. While SST influences daily and seasonal pCO_{2w} variability in the SAB (Signorini et al., 2013; Xue et al., 2016), we find no statistically significant change over the time series in SST or pCO_{2t} (Fig. 2B and C), therefore the change is likely due only to pCO_{2nt}. Since neither of the variables associated with mixing, Altamaha River stream flow and SSS, exhibit statistically significant increases, we can conclude from the available observations that the increasing river DIC concentration, and possibly the DIC flux from rivers and marshes to the SAB, is a potential source for increasing pCO_{2w} at the GR mooring (Fig. 3A; Table 1). There is no evidence of changes in biological production (Chl *a*) at the GR mooring, however, without an estimate for biological respiration or net primary production, we cannot estimate the potential role of DIC produced on the inner shelf.

As a result of increased pCO_{2w}, which is greater than the atmospheric increase, ΔpCO_2 and FCO_2 are also increasingly more positive and could result in a decreased annual net sink. These results are consistent with findings on the Scotia Shelf, North America, which is an increasing net source of CO_2 to the atmosphere (Shadwick et al., 2010). The pCO_{2a} increase at the GR mooring likely contributes up to ~2.0 μatm y^{-1} of the overall pCO_{2w} increase, however, other sources must account for the remaining portion. Based on the elimination of factors, such as a lack of increasing trends in SSS, SST, and Chl *a*, we suggest that further investigation into the shelf DIC and net biological processes in the coastal marshes and rivers could help resolve the source of increased GR mooring pCO_{2w}.

Compared with open ocean pCO_{2w}, coastal pCO_{2w}, and its variability, are more strongly influenced by terrestrial export and episodic events, such as storm induced vertical mixing over a shallow water column or mixed layer, than in the open ocean (Gledhill et al., 2015). The confidence interval associated with the pCO_{2w} increase over ~8.5 years at the GR mooring is greater than those reported for open ocean sites in the Atlantic (Bates et al., 2014, 2012; Fay and McKinley, 2013; McKinley et al., 2011), and could be interpreted as higher coastal zone variability compared with the open ocean. The observed trend variability is also likely influenced by the start and end dates of the time series; that is the time series starts during a dry period and ends during a wet period. Episodic events, such as wet periods (e.g., 2009–2010), drought periods (e.g., 2012), and tropical cyclones (surface water cooling or mixing) in the southeast USA (Crosswell et al., 2014) can all contribute to large trend variability. In Section 5.1 we assessed the influence of lateral materials flux via river stream flow, though apart from river stream flow, other extreme mixing variations could transport upwelled oceanic cold intrusions onshore (see Section 5.3). Episodic events increase variability and make it challenging to determine the underlying mechanisms that control sub-decadal trends; however, a greater understanding of mixing at the GR mooring could constrain this particular uncertainty. Finally, carrying the time series out to over two decades could also decrease the overall trend and its variability (Fay and McKinley, 2013), which highlights the necessity of continued observations at this and other coastal moorings.

4.4. Net annual FCO_2 source-sink variability

Considering the data loss during most years, if we only compare years with minimal data loss (2008, 2010, and 2012; Table 2), then there is still no consensus on whether this site is consistently a source or a sink. Rather, the site is highly variable and there is still a great amount of uncertainty surrounding the annual FCO_2 (Fig. 5). As we find for year 2012, a previous assessment of the SAB in 2005 and 2006 also determined that the inner shelf could be a source of CO_2 to the atmosphere (Jiang et al., 2008b). The observed interannual variability and uncertainty in FCO_2 in this work, and differences with estimates from previous studies of the SAB, could be due the complex hydrographic regime at the boundary of the inner and middle shelf where the GR mooring is located (Castelao, 2011; Menzel, 1993; Signorini and McClain, 2007). Whether the region represented by the GR mooring is an annual source or sink is determined by the hydrography, including extent of the freshwater plume, the location of the Gulf Stream, and/or Gulf Stream-induced upwellings. For example, decreased river stream flow (year 2012) could contribute by increasing the residence time of water on the inner shelf (Menzel, 1993), thus allowing for a longer period of time over which laterally transported OM, and subsequently respiration, could remain on the inner shelf near the GR mooring and enhance pCO_{2nt} (Fig. 3). Another example, during 2007 transport/Gulf Stream-induced upwelling of lower SST waters with higher TA and nutrient concentrations than shelf waters, could have decreased pCO_{2w}, which could lead to negative FCO_2, while providing nutrients for Chl *a* increases (Signorini et al., 2013). A short term return to negative FCO_2 accompanied by a decrease in SST during the later spring in 2007 could be evidence of the effects of onshelf transport, thus the observed decreases in pCO_{2t} and pCO_{2nt} with a several month increase in Chl *a* (Figs. 2B & C, 3B, and 4A–C). Even short-term hydrographic changes could impact annual sums and uncertainty, though a more thorough understanding of the mixing regime at the GR mooring is need to better assess the quantitative impacts on interannual FCO_2 and the alternating source/sink.

Another factor that could contribute to large uncertainties in annual FCO_2 is the use of various gas transfer velocity estimates. We find that our estimates using two different FCO_2 parameterizations do not always agree on the sign of FCO_2 (Fig. 5). For example, the W09 hybrid model closely resembles a quadratic function, which shows larger differences at higher winds speeds compared with the MG01 cubic function, and there are also slight differences in the intercepts (Eqs. (4) and (5)). For years with a greater number of days with higher U_{10}, this may be an important distinction and is likely a key source for daily to interannual uncertainty since at higher wind speeds there are greater differences between the resulting fluxes (Fig. 4A and B). The large error bars (annual uncertainty) in Fig. 5 are due to accumulation of uncertainty (daily variability in pCO_{2w}). Furthermore, from a methodological standpoint, larger data gaps in 2007, 2009, 2011, 2013, and 2014 (see Table 2 for the number of missing days in each year) will also affect annual fluxes. For comparison, the Jiang et al. (2008a) study presented estimates using a quadratic wind speed relationship with a zero intercept (Wanninkhof, 1992), thus, the results of the present study should generally be comparable; therefore methodologies between studies are not likely contributing to differences in our source/sink estimates. In general, the alternating annual source-sink and disagreement between the FCO_2 parameterizations at the site has implications for estimating annual carbon budgets in this region and could contribute to overall regional budget uncertainties.

5. Conclusions

We have shown that $MAPCO_2$ system, underway, and calculated pCO_{2w} from discrete water samples at the GR mooring are in reasonably good agreement, even though the majority of the cruise observations compiled over the time series of the GR mooring were not collected using rigorously established internal consistency methods (best practices). While there are some discrepancies in the validation results, general uncertainties associated with the method can be quantified, thus improving data synthesis. We recommend that samples collected for internal consistency should be collected as close to the mooring equilibrator intake as possible and within minutes of the $MAPCO_2$ system observation. If samples cannot be analyzed immediately while the cruise is underway, then they should be treated and stored according to established protocols and analyzed as soon as possible (Dickson et al., 2007). While DIC and TA are the most commonly and easily collected and analyzed carbonate system variables, this pairing may not be the most accurate or precise method for calculating pCO_{2w}, especially on highly variable ocean margins influenced by lower SSS waters. The broader implications for validation and time series assessments will allow future studies to merge the methods for determining pCO_{2w} variability explored here, and can also contribute to discerning the biogeochemical drivers of CO_2 on highly variable coastal margins.

SST is an important source of daily to seasonal pCO_{2w} and FCO_2 variability; however, longer term increases in pCO_{2w} are likely driven by pCO_{2nt} at the GR mooring. The combined effects of all non-thermal processes (net biological processes, air-sea exchange, and transport) likely contribute to the increase in pCO_{2nt}, thus pCO_{2w}. Further work is needed to calculate time series of DIC and TA at the GR mooring, which can be used in biogeochemical models to determine the contributions of mixing, biological processes, and gas exchange.

Depending on the parameterization used, the net annual FCO_2 at the GR mooring can have large differences in the source-sink term and can also vary greatly year-to-year. According to the estimates presented here, the majority of the time the GR mooring site is a sink for atmospheric CO_2, though the mixing regime likely plays an important role in annual estimates, which we have yet to discern. The results of the present study differ from previous estimates, which were based on seasonal cruises and interpolation rather than a continuous time series, assuming that the GR mooring is a good representation of the SAB inner shelf. There appears to be a clear need to re-evaluate FCO_2 on the entire shelf, as well as determine the biogeochemical processes that influence pCO_{2w}.

Acknowledgements

The Gray's Reef CO_2 mooring effort has been supported initially by the National Oceanic and Atmospheric Administration's Global Carbon Cycle (NOAA-GCC) and now NOAA – Ocean Acidification Program (OAP) via the South East Coastal Ocean Observing Regional Association (SECOORA); co-operative agreement number: NA11NOS0120033. JJR's time has been supported by both NOAA OAP (through SECOORA) and a University of Delaware Internal Fund (to WJC). XH is supported by Texas Research Development Fund. LX thanks the China Scholarship Council for providing the state scholarship fund (No. 201404180014). We thank the Georgia Coastal Ecosystems Long Term Ecological Research network for assistance in ground-truthing the mooring. Our late colleague Yongchen Wang was instrumental in the initial deployment of the mooring sensors and for ground-truthing the sensor data. Finally, we thank Sarah Fangman, Jared Halonen, Todd Recicar, and Randy Rudd at the Gray's Reef National Marine Sanctuary for providing vessel and diver support to help maintain the mooring operation. The authors also thank Dr. Todd Martz for very useful comments on an early version of this manuscript. This is PMEL contribution 4289 and JISAO contribution 2414. WJC would also like to thank NASA support on coastal carbon synthesis efforts (NNX11AD47G).

All observations used in this research are available to the public through the Carbon Dioxide Information Analysis Center (CDIAC; http://cdiac.ornl.gov/), the National Center for Environmental Information (https://www.nodc.noaa.gov/oceanacidification/stewardship/data_portal.html), the NASA Giovanni Server (http://disc.sci.gsfc.nasa.gov/giovanni), and the Georgia Coastal Ecosystems Long Term Research Network (http://gce-lter.marsci.uga.edu/portal/usgs_doctortown/historic/data/index.xml).

Appendix A. Supporting information

Supplementary data associated with this article can be found in the online version at doi:10.1016/j.csr.2017.06.022.

References

Bates, N., Astor, Y., Church, M., Currie, K., Dore, J., González-Davila, M., Lorenzoni, L., Muller-Karger, F., Olafsson, J., Santana-Casiano, J., 2014. A time-series view of changing ocean chemistry due to ocean uptake of anthropogenic CO_2 and ocean acidification. Oceanography 27, 126–141.

Bates, N.R., Best, M.H.P., Neely, K., Garley, R., Dickson, A.G., Johnson, R.J., 2012. Detecting anthropogenic carbon dioxide uptake and ocean acidification in the North Atlantic Ocean. Biogeosciences 9, 2509–2522.

Bauer, J.E., Cai, W., Raymond, P.A., Bianchi, T.S., Hopkinson, C.S., Regnier, P.A.G., 2013. The changing carbon cycle of the coastal ocean. Nature 504, 61–70.

Blanton, J., Atkinson, P., 1983. Transport and fate of river discharge on the continental shelf of the Southeastern United States. J. Geophys. Res. 88, 4730–4738.

Boehme, S.E., Sabine, C.L., Reimers, C.E., 1998. CO_2 fluxes from a coastal transect: a time-series approach. Mar. Chem. 63, 49–67.

Cai, W.-J., 2011. Estuarine and coastal ocean carbon paradox: CO_2 sinks or sites of terrestrial carbon incineration? Ann. Rev. Mar. Sci. 3, 123–145.

Cai, W.-J., Hu, X., Huang, W.-J., Murrell, M.C., Lehrter, J.C., Lohrenz, S.E., Chou, W.-C., Zhai, W., Hollibaugh, J.T., Wang, Y., Zhao, P., Guo, X., Gundersen, K., Dai, M., Gong, G.-C., 2011. Acidification of subsurface coastal waters enhanced by eutrophication. Nat. Geosci. 4, 766–770.

Cai, W.-J., Wang, Y., 1998. The chemistry, fluxes, and sources of carbon dioxide in the estuarine waters of the Satilla and Altamaha Rivers, Georgia. Limnol. Oceanogr. 43, 657–668.

Cai, W.-J., Wang, Z.A., Wang, Y., 2003. The role of marsh-dominated heterotrophic continental margins in transport of CO_2 between the atmosphere, the land-sea interface and the ocean. Geophys. Res. Lett. 30, 1–4.

Castelao, R., 2011. Intrusions of Gulf Stream waters onto the South Atlantic Bight shelf. J. Geophys. Res., 116.

Castelao, R.M., 2014. Mesoscale eddies in the South Atlantic Bight and the Gulf Stream Recirculation region: vertical structure. J. Geophys. Res. Ocean. 119, 2048–2065.

Castelao, R.M., He, R., 2013. Mesoscale eddies in the South Atlantic Bight. J. Geophys. Res. Ocean. 118, 5720–5731.

Crosswell, J.R., Wetz, M.S., Hales, B., Paerl, H.W., 2014. Extensive CO_2 emissions from shallow coastal waters during passage of Hurricane Irene (August 2011) over the Mid-Atlantic coast of the U.S.A.. Limnol. Oceanogr. 59, 1651–1665.

Dickson, A.G., Millero, F.J., 1987. A comparison of the equilibrium constants for the dissociation of carbonic acid in seawater media. Deep Sea Res. A. Oceanogr. Res. Pap. 34, 1733–1743.

Dickson, A.G., Sabine, C.L., Christian, J.R., 2007. Guide to Best Practices for Ocean CO_2 Measurements 3. PICES Special Publication.

Fay, A.R., McKinley, G.A., 2013. Global trends in surface ocean pCO_2 from in situ data. Glob. Biogeochem. Cycles 27, 541–557.

Feely, R.A., Sabine, C.L., Lee, K., Berelson, W., Kleypas, J., Fabry, V.J., Millero, F.J., 2004. Impact of anthropogenic CO_2 on the CaCO3 system in the oceans. Science 305, 362–366.

Feely, R.A., Sabine, C.L., Hernandez-ayon, J.M., Ianson, D., Hales, B., 2008. Evidence for upwelling of corrosive "acidified" water onto the continental shelf. Science 320, 1490–1492.

Gledhill, D.K., White, M.M., Salisbury, J., Thomas, H., Mlsna, I., Liebman, M., Mook, B., Grear, J., Candelmo, A.C., Chambers, R.C., Gobler, C.J., Hunt, C.W., King, A.L., Price, N.N., Signorini, S.R., Stancioff, E., Stymiest, C., Wahle, R.A., Waller, J.D., Rebuck, N.D., Wang, Z.A., 2015. Ocean and coastal acidification off New England and Nova Scotia. Oceanography 28, 182–197.

Huang, W.-J., Cai, W.-J., Castelao, R.M., Wang, Y., Lohrenz, S.E., 2013. Effects of a wind-driven cross-shelf large river plume on biological production and CO_2 uptake on the Gulf of Mexico during spring. Limnol. Oceanogr. 58, 1727–1735.

Huang, W.-J., Wang, Y., Cai, W.-J., 2012. Assessment of sample storage techniques for total alkalinity and dissolved inorganic carbon in seawater. Limnol. Oceanogr. Methods 10, 711–717.

Jiang, L.-Q., Cai, W.-J., Wang, Y., 2008a. A comparative study of carbon dioxide degassing in river- and marine-dominated estuaries. Limnol. Oceanogr. 53, 2603–2615.

Jiang, L.-Q., Cai, W.-J., Wang, Y., Bauer, J.E., 2013. Influence of terrestrial inputs on continental shelf carbon dioxide. Biogeosciences 10, 1–22.

Jiang, L.-Q., Cai, W.-J., Wang, Y., Diaz, J., Yager, P.L., Hu, X., 2010. Pelagic community respiration on the continental shelf off Georgia, USA. Biogeochemistry 98, 101–113.

Jiang, L.-Q., Cai, W.-J., Wanninkhof, R., Wang, Y., Lüger, H., 2008b. Air-sea CO_2 fluxes on the U.S. South Atlantic Bight: spatial and seasonal variability. J. Geophys. Res. 113, C07019.

Le Quere, C., Andrew, R.M., Canadell, J.G., Sitch, S., Ivar Korsbakken, J., Peters, G.P., Manning, A.C., Boden, T.A., Tans, P.P., Houghton, R.A., Keeling, R.F., Alin, S., Andrews, O.D., Anthoni, P., Barbero, L., Bopp, L., Chevallier, F., Chini, L.P., Ciais, P., Currie, K., Delire, C., Doney, S.C., Friedlingstein, P., Gkritzalis, T., Harris, I., Hauck, J., Haverd, V., Hoppema, M., Klein Goldewijk, K., Jain, A.K., Kato, E., Kortzinger, A., Landschutzer, P., Lefevre, N., Lenton, A., Lienert, S., Lombardozzi, D., Melton, J.R., Metzl, N., Millero, F., Monteiro, P.M.S., Munro, D.R., Nabel, J.E.M.S., Nakaoka, S.I., O'Brien, K., Olsen, A., Omar, A.M., Ono, T., Pierrot, D., Poulter, B., Rodenbeck, C., Salisbury, J., Schuster, U., Schwinger, J., Seferian, R., Skjelvan, I., Stocker, B.D., Sutton, A.J., Takahashi, T., Tian, H., Tilbrook, B., Van Der Laan-Luijkx, I.T., Van Der Werf, G.R., Viovy, N., Walker, A.P., Wiltshire, A.J., Zaehle, S., 2016. Global carbon budget 2016. Earth Syst. Sci. Data 8, 605–649.

Lee, K., Kim, T.W., Byrne, R.H., Millero, F.J., Feely, R.A., Liu, Y.M., 2010. The universal ratio of boron to chlorinity for the North Pacific and North Atlantic oceans. Geochim. Cosmochim. Acta 74, 1801–1811.

Lewis, E., Wallace, D., 1998. Program developed for CO_2 system calculations. ORNL/CDIAC 105, Carbon Dioxide Information Analysis Center. Oak Ridge National Laboratory US Department of Energy, Oak Ridge, Tennessee.

McGillis, W.R., Edson, J.B., Hare, J.E., Fairall, C.W., 2001. Direct covariance air-sea CO_2 fluxes. J. Geophys. Res. 106, 16729–16745.

McKinley, G.A., Fay, A.R., Takahashi, T., Metzl, N., 2011. Convergence of atmospheric and North Atlantic carbon dioxide trends on multidecadal timescales. Nat. Geosci. 4, 606–610.

Mehrbach, C., Culberson, C.H., Hawley, J.E., Pytkowicz, R.M., 1973. Measurement of the apparent dissociation constants of carbonic acid in seawater at atmospheric pressure. Limnol. Oceanogr. 18, 897–907.

Menzel, D., 1993. Ocean processes: US southeast continental shelf. US Dep. Energy, Off. Tech. Inf. DOE/OSTI-1, 121.

Michalak, A.M., Jackson, R.B., Marland, G., Sabine, C.L., Group, C.C.W., 2011. A U.S. Carbon Cycle Science Plan. Nova Science Publishers, Inc.

Newton, J.A., Feely, R.A., Jewett, E.B., Williamson, P., Mathis, J., 2014. Global ocean acidification observing network: requirements and governance plan.

Patsavas, M.C., Byrne, R.H., Wanninkhof, R., Feely, R.A., Cai, W.-J., 2015. Internal consistency of marine carbonate system measurements and assessments of aragonite saturation state: insights from two U.S. coastal cruises. Mar. Chem. 176, 9–20.

Pierrot, D., Neill, C., Sullivan, K., Castle, R., Wanninkhof, R., Lüger, H., Johannessen, T., Olsen, A., Feely, R.A., Cosca, C.E., 2009. Recommendations for autonomous underway pCO_2 measuring systems and data-reduction routines. Deep Sea Res. Part II Top. Stud. Oceanogr. 56, 512–522.

Pomeroy, L.R., Sheldon, J.E., Sheldon, W.M., Blanton, J.O., Amft, J., Peters, F., 2000. Seasonal changes in microbial processes in estuarine and continental shelf waters of the south-eastern USA. Estuar. Coast. Shelf Sci. 51, 415–428.

Ribas-Ribas, M., Rérolle, V.M.C., Bakker, D.C.E., Kitidis, V., Lee, G.A., Brown, I., Achterberg, E.P., Hardman-Mountford, N.J., Tyrrell, T., 2014. Intercomparison of carbonate chemistry measurements on a cruise in northwestern European shelf seas. Biogeosciences 11, 4339–4355.

Sabine, C.L., Feely, R.A., Gruber, N., Key, R.M., Lee, K., Bullister, J.L., Wanninkhof, R., Wong, C.S., Wallace, D.W.R., Tilbrook, B., Millero, F.J., Peng, T.-H., Kozyr, A., Ono, T., Rios, A.F., 2004. The oceanic sink for anthropogenic CO_2. Science 305, 367–371.

Schaefer, S.C., Alber, M., 2007. Temporal and spatial trends in nitrogen and phosphorus inputs to the watershed of the Altamaha River, Georgia, USA. Biogeochemistry 86, 231–249.

Schar, D., Atkinson, M., Johengen, T., Pinchuk, A., Purcell, H., Robertson, C., Smith, G. J., Tamburri, M., 2010. Performance demonstration statement PMEL MAPCO2/

Battelle Seaology pCO_2 monitoring system.
Shadwick, E.H., Thomas, H., Azetsu-Scott, K., Greenan, B.J.W., Head, E., Horne, E., 2011. Seasonal variability of dissolved inorganic carbon and surface water pCO_2 in the Scotian Shelf region of the Northwestern Atlantic. Mar. Chem. 124, 23–37.
Shadwick, E.H., Thomas, H., Comeau, A., Craig, S.E., Hunt, C.W., Salisbury, J.E., 2010. Air-Sea CO_2 fluxes on the Scotian Shelf: seasonal to multi-annual variability. Biogeosciences 7, 3851–3867.
Sheldon, J.E., Alber, M., 2013. Effects of Climate Signals on River Discharge to Ossabaw, St. Andrew, and Cumberland Sounds. Georgia Coastal Reseach Council.
Sheldon, J.E., Burd, A.B., 2013. Alternating effects of climate drivers on Altamaha river discharge to coastal Georgia, USA. Estuaries Coasts 37, 772–788.
Signorini, S.R., Mannino, A., Najjar, R.G., Friedrichs, M.A.M., Cai, W.-J., Salisbury, J., Wang, Z.A., Thomas, H., Shadwick, E., 2013. Surface ocean pCO_2 seasonality and sea-air CO_2 flux estimates for the North American east coast. J. Geophys. Res. Ocean. 118, 5439–5460.
Signorini, S.R., McClain, C.R., 2007. Large-scale forcing impact on biomass variability in the South Atlantic Bight. Geophys. Res. Lett. 34, L21605.
Sunda, W.G., Cai, W.-J., 2012. Eutrophication induced CO_2-acidification of subsurface coastal waters: interactive effects of temperature, salinity, and atmospheric pCO_2. Environ. Sci. Technol. 46, 10651–10659.
Sutton, A.J., Sabine, C.L., Feely, R.A., Cai, W.-J., Cronin, M.F., McPhaden, M.J., Morell, J.M., Newton, J.A., Noh, J.-H., Olafsdottir, S.R., Salisbury, J.E., Send, U., Vandemark, D.C., Weller, R.A., 2016. Using present-day observations to detect when anthropogenic change forces surface ocean carbonate chemistry outside pre-industrial bounds. Biogeosciences Discuss., 1–30.
Sutton, A.J., Sabine, C.L., Maenner-Jones, S., Lawrence-Slavas, N., Meinig, C., Feely, R. a., Mathis, J.T., Musielewicz, S., Bott, R., McLain, P.D., Fought, J., Kozyr, A., 2014. A high-frequency atmospheric and seawater pCO_2 data set from 14 open ocean sites using a moored autonomous system. Earth Syst. Sci. Data Discuss. 7, 385–418.
Takahashi, T., Olafsson, J., Goddard, J., Chipman, D., Sutherland, S., 1993. Seasonal variation of CO_2 and nutrients in the high-latitude surface oceans: a comparative study. Glob. Biogeochem. Cycles 7, 843–878.
Takahashi, T., Sutherland, S.C., Chipman, D.W., Goddard, J.G., Cheng, H., Newberger, T., Sweeney, C., Munro, D.R., 2014. Climatological distributions of pH, pCO_2, total CO_2, alkalinity, and $CaCO_3$ saturation in the global surface ocean, and temporal changes at selected locations. Mar. Chem. 164, 95–125.
Takahashi, T., Sutherland, S.C., Feely, R.A., Wanninkhof, R., 2006. Decadal change of the surface water pCO_2 in the North Pacific: a synthesis of 35 years of observations. J. Geophys. Res. Ocean. 111, 1–20.
Takahashi, T., Sutherland, S.C., Sweeney, C., Poisson, A., Metzl, N., Tilbrook, B., Bates, N., Wanninkhof, R., Feely, R.A., Sabine, C., Olafsson, J., Nojiri, Y., 2002. Global sea–air CO_2 flux based on climatological surface ocean pCO_2, and seasonal biological and temperature effects. Deep Sea Res. Part II Top. Stud. Oceanogr. 49, 1601–1622.
Thomas, H., Friederike Prowe, A.E., van Heuven, S., Bozec, Y., de Baar, H.J.W., Schiettecatte, L.-S., Suykens, K., Koné, M., Borges, A.V., Lima, I.D., Doney, S.C., 2007. Rapid decline of the CO_2 buffering capacity in the North Sea and implications for the North Atlantic Ocean. Glob. Biogeochem. Cycles 21, 1–13.
Tseng, C.-M., Wong, G.T.F., Chou, W.-C., Lee, B.-S., Sheu, D.-D., Liu, K.-K., 2007. Temporal variations in the carbonate system in the upper layer at the SEATS station. Deep Sea Res. Part II Top. Stud. Oceanogr. 54, 1448–1468.
Van Heuven, S., Pierrot, D., Lewis, E., Wallace, D.W.R., 2009. MATLAB Program Developed for CO_2 System Calculations. Oak Ridge, Tennessee.
Vandemark, D., Salisbury, J.E., Hunt, C.W., Shellito, S.M., Irish, J.D., McGillis, W.R., Sabine, C.L., Maenner, S.M., 2011. Temporal and spatial dynamics of CO_2 air-sea flux in the Gulf of Maine. J. Geophys. Res. 116, C01012.
Wang, Z.A., Wanninkhof, R., Cai, W.-J., Byrne, R.H., Hu, X., Peng, T.-H., Huang, W.-J., 2013. The marine inorganic carbon system along the Gulf of Mexico and Atlantic coasts of the United States: insights from a transregional coastal carbon study. Limnol. Oceanogr. 58, 325–342.
Wanninkhof, R., 1992. Relationship between wind speed and gas exchange over the ocean. J. Geophys. Res. - Ocean. 97, 7373–7382.
Wanninkhof, R., 2014. Relationship between wind speed and gas exchange over the ocean revisited. Limnol. Oceanogr. Methods 12, 351–362.
Wanninkhof, R., Asher, W.E., Ho, D.T., Sweeney, C., McGillis, W.R., 2009. Advances in quantifying air-sea gas exchange and environmental forcing. Annu. Rev. Mar. Sci. 1, 213–244.
Wanninkhof, R., Barbero, L., Byrne, R., Cai, W.J., Huang, W.J., Zhang, J.Z., Baringer, M., Langdon, C., 2015. Ocean acidification along the Gulf Coast and East Coast of the USA. Cont. Shelf Res. 98, 54–71.
Wanninkhof, R., Park, G.-H., Takahashi, T., Sweeney, C., Feely, R., Nojiri, Y., Gruber, N., Doney, S.C., McKinley, G.A., Lenton, A., Le Quéré, C., Heinze, C., Schwinger, J., Graven, H., Khatiwala, S., 2013. Global ocean carbon uptake: magnitude, variability and trends. Biogeosciences 10, 1983–2000.
Xue, L., Cai, W.J., Hu, X., Sabine, C., Jones, S., Sutton, A.J., Jiang, L.Q., Reimer, J.J., 2016. Sea surface carbon dioxide at the Georgia time series site (2006–2007): air-sea flux and controlling processes. Prog. Oceanogr. 140, 14–26.
Yang, B., Byrne, R.H., Lindemuth, M., 2015. Contributions of organic alkalinity to total alkalinity in coastal waters: a spectrophotometric approach. Mar. Chem. 176, 199–207.
Yoder, J.A., Atkinson, L.P., Bishop, S.S., Blanton, J.O., Lee, T.N., Pietrafesa, L.J., 1985. Phytoplankton dynamics within Gulf Stream intrusions on the southeastern United States continental shelf during summer 1981. Cont. Shelf Res. 4, 611–635.